

# Multiwatt continuous wave Nd:KGW laser with hot-band diode pumping

RUBEL CHANDRA TALUKDER, MD. ZUBAER EIBNA HALIM, TANANT WARITANANT, AND ARKADY MAJOR\*

Department of Electrical and Computer Engineering, University of Manitoba, Winnipeg R3T 5V6, Canada

\*Corresponding author: a.major@umanitoba.ca

Received 21 June 2016; accepted 15 July 2016; posted 21 July 2016 (Doc. ID 268828); published 8 August 2016

We have demonstrated what we believe is the first continuous wave neodymium-doped potassium gadolinium tungstate crystal (Nd:KGW) laser with hot-band diode pumping at  $\sim 910$  nm. This pumping wavelength reduced the quantum defect by  $>46\%$  as compared to conventional  $\sim 810$  nm pumping and resulted in significantly lower thermal lensing. The laser produced 2.9 W of average output power at 1067 nm in a diffraction-limited beam for an absorbed pump power of 8.3 W. The slope efficiency and optical-to-optical efficiency were found to be 43% and 35%, respectively. Significant reduction of quantum defect offered by this pumping wavelength and availability of suitable high-power laser diodes opens up an attractive way to further power and efficiency scaling of Nd:KGW lasers. © 2016 Optical Society of America

**OCIS codes:** (140.3480) Lasers, diode-pumped; (140.3530) Lasers, neodymium; (140.3580) Lasers, solid-state.

<http://dx.doi.org/10.1364/OL.41.003810>

Neodymium-doped potassium gadolinium tungstate crystal (Nd:KGW) is one of the most effective active media for solid-state laser engineering in the near-infrared region. Nd:KGW has some exceptional properties compared with other widely used Nd<sup>3+</sup>-doped laser crystals operating around 1  $\mu\text{m}$ , such as Nd:YAG and Nd:YVO. High doping concentration of Nd<sup>3+</sup> ion and high slope efficiency can be achieved with it [1]. This crystal is well known for its high emission cross section (higher than that of Nd:YAG) and thus efficient continuous wave (CW) [2], Q-switched [3], and mode-locked operation [4,5]. In addition, birefringence of the host results in strongly polarized emission, which is advantageous for further frequency conversion [6–8]. Because of the high third-order nonlinearity of the host [9], Nd:KGW crystals and lasers are widely used to generate multiple wavelengths via stimulated Raman scattering [6,7]. CW Raman lasing based on Nd:KGW crystal was also reported [10].

Unfortunately, the relatively low thermal conductivity (about half that of Nd:YVO) of KGW host crystals and large quantum defect (with  $\sim 810$  nm pumping) lead to significant thermo-optical distortions. As a result of thermal effects, power scaling to the multiwatt level is hindered [11]. Therefore,

reduction of thermal lensing is the key strategy to achieve power scaling. This can be done by pumping at longer wavelengths (as compared to traditional 808 nm) to reduce the quantum defect. Although pumping at around 880 nm was reported [12–14], this is not the longest possible pump wavelength for Nd-ion-based gain media. Recently, efficient diode pumping (at 914 nm) of a Nd:YVO laser from the highest thermally populated sublevel (i.e., hot band) of the ground-state manifold was realized, thus enabling slope efficiency to reach up to 81% in the CW [15] regime and up to 77% in the mode-locked regime [16]. It was also shown that such long wavelength pumping reduced thermal lensing by a factor of 2 [17] in comparison with 808 nm pump wavelength.

In this work, we demonstrate a multiwatt CW Nd:KGW laser by using a similar approach. A hot-band pumping wavelength of around 910 nm was used in the experiment. It reduced the quantum defect by  $>46\%$  when compared to traditional  $\sim 810$  nm pumping and enabled high-power operation of the Nd:KGW laser with 2.9 W of output power. Since high-power laser diodes around 910–920 nm are widely used for pumping of Yb-doped fiber lasers, the results of this work open a promising route to power scaling of Nd:KGW lasers.

Figure 1(a) shows a schematic of the energy level diagram of the Nd:KGW crystal. Electron transition from the lowest sublevel of the ground-state manifold  $^2I_{9/2}$  to the pump level  $^2F_{5/2} + ^2H_{9/2}$  corresponds to the 810 nm wavelength that is generally used for pumping of Nd:KGW crystals and other Nd-doped gain media.

To reduce the heat generated inside the crystal, in this work we used a pumping wavelength that corresponds to an electron excitation from the thermally populated highest sublevel of the ground-state manifold  $^4I_{9/2}$  to the upper laser level  $^4F_{3/2}$ , as shown in Fig. 1(a). To estimate the potential of Nd:KGW crystal for pumping at wavelengths longer than  $\sim 880$  nm (ground-state to the upper laser level  $^4F_{3/2}$  transition) we examined its fluorescence spectrum in this wavelength range, shown in Fig. 1(b). Since all sublevels of the ground-state manifold can be also used as quasi-three-level laser transitions, the emission and absorption peaks coincide [15]. Therefore, our motivation for using the 910 nm pumping wavelength shown in Fig. 1(a) came from the fluorescence data [18] where this transition is clearly resolved.

For CW operation, we have designed a five-mirror cavity, as shown in Fig. 2. An Ng-cut 20-mm-long Nd:KGW slab sample

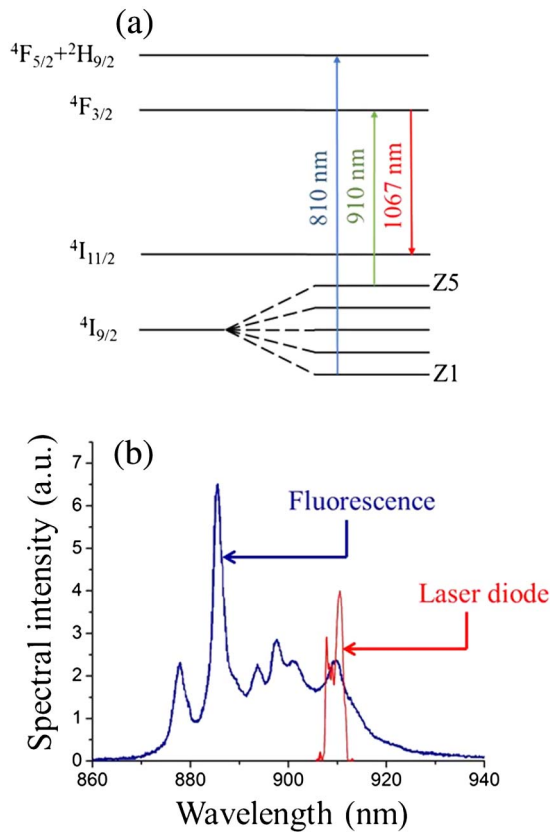


**Fig. 1.** (a) Energy level diagram of Nd:KGW and (b) its fluorescence spectrum for the Nm-polarization around 900 nm [18]. Pump diode spectrum is also shown.

with dimensions of 1.6 mm × 6 mm × 20 mm and 3 at. % doping concentration was used (Altechna). The crystal had flat end faces, which were antireflection (AR) coated at 1067 nm. Cavity mirrors M1–M4 were highly reflecting at 1067 nm. Cavity focusing mirrors M2 and M4 had 400 and 500 mm radii of curvature, respectively. M3 was a flat dichroic mirror. The best performance was achieved using an output coupler with 10% transmission. The distances L1, L2, L3, and L4 were 315, 455, 481, and 462 mm, respectively.

A high-power fiber-coupled laser diode (110 μm core, NA = 0.12) operating around 910 nm (~5 nm linewidth) was used as a pump source. The unpolarized output from the laser diode was first collimated with an  $f = 40$  mm collimator lens and subsequently focused onto the laser crystal by an

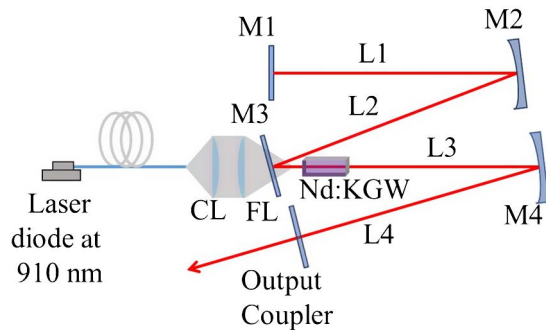


**Fig. 2.** Experimental setup for CW operation.

$f = 200$  mm focusing lens, producing a pump spot diameter of ~550 μm. The laser crystal was wrapped in indium foil to improve thermal interface between the crystal and the aluminum heat sink. The top and bottom surfaces of the crystal (6 mm × 20 mm) were in contact with the heat sink and water cooled at 16°C.

At 15 W of pump power, about 8.3 W was absorbed by the crystal and 2.9 W of average output power was generated at 1067 nm. For 6–15 W of pump power, the pump absorption varied from 55% to 71% of the input power because of the pump wavelength shift. The input–output power curve is displayed in Fig. 3(a). With respect to the absorbed pump power, the slope efficiency was found to be 43% and optical-to-optical efficiency reached 35%. Moderate pump absorption efficiency in our case can be enhanced by using a longer crystal with higher doping concentration or by using a wavelength-stabilized pump diode. In the case of ~810 nm pumping, the highest slope efficiency and optical-to-optical efficiency for Nd:KGW crystal were reported as 75% and 66%, respectively, with respect to the absorbed pump power [19,20]. The best slope efficiency for ~880 nm pumping was 66.4% with optical-to-optical efficiency reaching 63.8% [14]. The maximum possible slope efficiency with 910 nm pumping can be estimated to be 85%. We believe that, in our proof-of-principle experiment, the lower values of slope and optical efficiency can be explained by the higher intracavity losses introduced by a larger number of mirrors (two-mirror cavities were used in previous works) and fairly high reflectivity of the

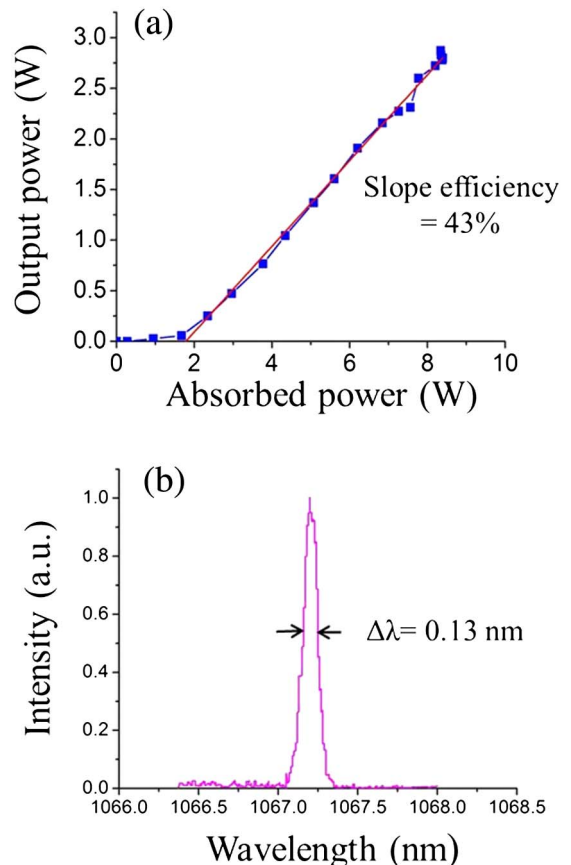


**Fig. 3.** (a) Measured output power with linear fit and (b) CW laser spectrum.

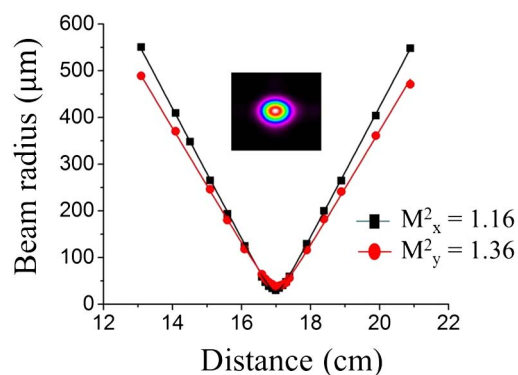


**Fig. 4.** Laser beam quality at 2.9 W of output power. Inset: transverse intensity profile of the laser beam.

crystal AR coatings at the laser wavelength, which was specified as 0.25% (per surface). Another contributing factor was that the output coupler used probably also did not have a completely optimal transmission.

The spectrum of the generated laser radiation is shown in Fig. 3(b). Its linewidth at half-maximum was measured to be 0.13 nm, limited by the resolution of our spectrometer (0.1 nm). The output laser radiation was linearly polarized along the Nm-axis.

The laser had excellent output beam quality. A CCD camera and a focusing lens of 150 mm were utilized for beam profiling. Beam quality factor  $M^2$  was found to be 1.16 in the horizontal direction and 1.36 in the vertical direction. The measurement data along with the output beam shape are presented in Fig. 4.

It is also instructive to compare the observed thermal lensing effect with all different reported pump wavelengths (i.e., 810, 880, and 910 nm). The thermal lens focusing power with 810 and 880 nm pumping was reported in [12]. At 810 nm pumping, it was measured to be  $\sim 9$  diopters in the horizontal direction and  $\sim 10$  diopters in the vertical direction with absorbed pump power of 2.35 W. The focusing power of the thermal lens for 880 nm pumping was also measured to have the same values in both directions at a higher absorbed pump power of 4.44 W. This result can be explained by the higher quantum defect for pumping with 810 nm wavelength as compared to pumping with 880 nm. In our experiment, the thermal lens dioptric power was measured using a modified ABCD matrix analysis that takes into account laser beam quality [21]. At 8.3 W of absorbed pump power, it was found to be  $\sim 5.5$  diopters in the horizontal direction and  $\sim 6.0$  diopters in the vertical direction. These measurements clearly indicate that even at the much higher absorbed pump power level the thermal lensing effect is significantly lower for 910 nm pumping as compared to both 880 and 810 nm pumping. Therefore, the proposed new pump wavelength at 910 nm holds strong potential for power scaling of Nd:KGW lasers owing to the strongly reduced thermal effects.

Although a lower thermal lensing in the case of 910 nm pumping is obvious, it is worth noting that direct comparison with the quoted values above is not straightforward because of

the different experimental conditions, such as the pump spot size, crystal geometry, pump absorption length, cooling geometry, and coolant temperature. Nonetheless, in the case of  $\sim 810$  nm pumping, a stronger thermal lensing by a factor of 2 should be observed in comparison with a 910 nm pump wavelength under the same experimental conditions [17].

In conclusion, multiwatt CW operation of a Nd:KGW at 1067 nm with hot-band diode pumping was demonstrated. To the best of our knowledge, this is the first time that this approach has been used with Nd:KGW laser crystal. The laser produced 2.9 W of average output power with excellent beam quality. The pump wavelength of  $\sim 910$  nm significantly ( $>46\%$ ) reduced quantum defect and, thus, the amount of heat deposited in the crystal. This opens up a way to further power scaling of Nd:KGW lasers by using high-power laser diodes that are currently widely used for pumping of Yb-doped fiber lasers.

**Funding.** Natural Sciences and Engineering Research Council of Canada (NSERC).

## REFERENCES

1. A. A. Demidovich, A. P. Shkadarevich, M. B. Danailov, P. Apai, T. Gasmi, V. P. Gribkovskii, A. N. Kuzmin, G. I. Ryabtsev, and L. E. Batay, *Appl. Phys. B* **67**, 11 (1998).
2. T. Graf and J. E. Balmer, *Opt. Eng.* **34**, 2349 (1995).
3. Y. Kalisky, L. Kravchik, and C. Labbe, *Opt. Commun.* **189**, 113 (2001).
4. A. Major, N. Langford, T. Graf, D. Burns, and A. I. Ferguson, *Opt. Lett.* **27**, 1478 (2002).
5. A. Major, N. Langford, T. Graf, and A. I. Ferguson, *Appl. Phys. B* **75**, 467 (2002).
6. A. S. Grabtchikov, A. N. Kuzmin, V. A. Lisinetskii, V. A. Orlovich, G. I. Ryabtsev, and A. A. Demidovich, *Appl. Phys. Lett.* **75**, 3742 (1999).
7. A. Major, J. S. Aitchison, P. W. E. Smith, N. Langford, and A. I. Ferguson, *Opt. Lett.* **30**, 421 (2005).
8. A. Major, D. Sandkuijl, and V. Barzda, *Opt. Express* **17**, 12039 (2009).
9. A. Major, J. S. Aitchison, P. W. E. Smith, F. Druon, P. Georges, B. Viana, and G. P. Aka, *Appl. Phys. B* **80**, 199 (2005).
10. A. A. Demidovich, A. S. Grabtchikov, V. A. Lisinetskii, V. N. Burakevich, V. A. Orlovich, and W. Kiefer, *Opt. Lett.* **30**, 1701 (2005).
11. P. A. Loiko, K. V. Yumashev, N. V. Kuleshov, and A. A. Pavlyuk, *Appl. Opt.* **49**, 6651 (2010).
12. K. Huang, W. Q. Ge, T. Z. Zhao, C. Y. Feng, J. Yu, J. G. He, H. Xiao, and Z. W. Fan, *Appl. Phys. B* **122**, 171 (2016).
13. A. J. Lee, H. M. Pask, D. J. Spence, and J. A. Piper, *Advanced Solid State Photonics*, OSA Technical Digest Series (Optical Society of America, 2010), paper ATuA22.
14. A. A. Bui, U. I. Dashkevich, V. A. Orlovich, and I. A. Khodasevich, *J. Appl. Spectrosc.* **82**, 578 (2015).
15. D. Sangla, M. Castaing, F. Balembos, and P. Georges, *Opt. Lett.* **34**, 2159 (2009).
16. T. Waritanant and A. Major, *Opt. Express* **24**, 12851 (2016).
17. T. Waritanant and A. Major, *Appl. Phys. B* **122**, 135 (2016).
18. R. Moncorge, B. Chambon, J. Y. Rivore, N. Garnier, E. Descroix, P. Laporte, H. Guillet, S. Roy, J. Mareschal, D. Pelenc, J. Doury, and P. Farge, *Opt. Mater.* **8**, 109 (1997).
19. G. Boulon, G. Metrat, N. Muhlstein, A. Brenier, M. R. Kokta, L. Kravchik, and Y. Kalisky, *Opt. Mater.* **24**, 377 (2003).
20. A. Abdolvand, K. G. Wilcox, T. K. Kalkandjiev, and E. U. Rafailov, *Opt. Express* **18**, 2753 (2010).
21. H. Mirzaei, S. Manjooan, and A. Major, *Proc. SPIE* **9288**, 928802 (2014).